



Effect of solvent polarity on the regioselective hydroxyalkylation of indole with trifluoroacetaldehyde hemiacetals

Swarada Peerannawar¹ · Abha Sood² · Alicia Brown² · Christian Schäfer¹ · Judith Alonzo¹ · Steven Sutton² · Matthew Christianson² · Raven Stocking² · Nicole Naclerio² · Béla Török¹ · Shainaz M. Landge²

Received: 10 May 2019 / Accepted: 25 June 2019
© Springer Science+Business Media, LLC, part of Springer Nature 2019

Abstract

The effect of solvents has been found as a crucial factor in determining the regioselectivity of the hydroxyalkylation of indole with trifluoroacetaldehyde hemiacetals. The appropriate selection of the solvent ensured to achieve absolute N1 or C3 regio/chemoselectivity of the reaction depending on the polarity and dielectric constant of the medium. Reaction conditions were optimized considering the effect of solvent, including temperature, time, and molar ratio of reactants to base. In order to rationalize this effect, density functional theory has been employed in which implicit as well as explicit role of solvent was studied, which were further validated with in situ ¹H NMR spectroscopy experiments. The comparison of transition states derived from the implicit calculations revealed that the lowest energy path of the reaction in dimethyl sulfoxide (DMSO) leads to product formation with N-selectivity. Further DFT calculations on explicit interactions of indole with DMSO indicated enhanced nucleophilicity on the N atom compared to that of C3 atom, which is evident from the calculated electrostatic potential (ESP) fit charges of these complexes. These findings appear to support the experimental data and explain the N-selectivity in DMSO.

Keywords Indoles · Organofluorine · Solvent effect · ¹H NMR spectroscopy · DFT calculations · Regioselective · Chemoselective · Solvent-substrate interaction · Modeling

Introduction

Organofluorine compounds are of primary importance in pharmaceutical and agrochemical applications as well as in the synthesis of advanced materials. Their significance is shown by the high volume of applications; e.g., an estimated 20% of the drugs contain at least one fluorine atom, in addition to their use as coating (Teflon) or fuel-cell membranes (Nafion) [1, 2].

Incorporating fluorine or a perfluoroalkyl group into the drug candidates can enhance their affinity towards biological targets and increase their metabolic stability, bioavailability, and membrane permeability. Indole derivatives represent a large family of compounds which are ubiquitously distributed in nature (alkaloids and peptides). These compounds are predominantly biologically active and serve as a core in many potential pharmaceutical leads [3, 4]. Functionalization of the indole moiety with a trifluoromethyl group can further enhance its drug-like potential [5–13]. The indole skeleton appears in several important classes of pharmaceutical scaffolds acting as anticancer, antiviral, antifungal, and antidiabetic agents. In addition, they have been evaluated against potential targets associated with neurodegenerative diseases such as Prion [14] or Alzheimer's disease [15]. Indoles most commonly undergo substitution reactions at their N1, C2, or C3 positions. There are numerous methods reported for the synthesis of C3-substituted indoles [16–19], which is the most reactive position in aromatic electrophilic substitutions. In contrast, developing selective methods for the N1 or C2 substitution is difficult [20, 21]. Direct N-alkylation, the most attractive method to obtain N-substituted derivatives, involves the initial formation of indolyl

Electronic supplementary material The online version of this article (<https://doi.org/10.1007/s11224-019-01386-x>) contains supplementary material, which is available to authorized users.

- ✉ Béla Török
bela.torok@umb.edu
- ✉ Shainaz M. Landge
slandge@georgiasouthern.edu

¹ Department of Chemistry, University of Massachusetts Boston, 100 Morrissey Blvd., Boston, MA, USA

² Department of Chemistry and Biochemistry, Georgia Southern University, 521 College of Education Drive, Statesboro, GA 30460-8064, USA

anion, but due to its ambident nature, both N- and C-alkylated products are formed. The nitrogen atom can be made the most reactive nucleophilic site only by deprotonation; thus, procedures for N-substitution commonly involve base-catalyzed nucleophilic substitution or conjugate addition reactions [22, 23]. As a result, the number of broadly applicable procedures for the synthesis of N-alkylated indole derivatives is limited [24]. The regioselectivity between the reactive centers can be delicately influenced by a number of factors, e.g., using different metal counter ions, application of metal [25] or phase transfer catalyst [26], addition of various bases [27], and solvents [28]. These traditional methods, however, carry several disadvantages such as harsh conditions, require molar equivalent of base, and often occur via multistep synthesis [29]. Recently, we have developed a selective microwave-assisted synthetic protocol that is able to yield a broad range of N-hydroxyalkated indoles [15, 30]. The often exclusive N-selectivity is fundamentally based on the use of polar, aprotic solvents, such as DMF and dimethyl sulfoxide (DMSO). However, the theoretical foundation of the solvent effect has been unclear. Herein, we report a mechanistic study involving experimental and theoretical investigations of this specific solvent effect which can accomplish the highly regioselective alkylation of indole either at its N1 (A) or C3 (B) position (Scheme 1).

Methods

Materials

All chemicals and reactants (indole, trifluoroacetaldehyde ethyl and methyl hemiacetals, triethylamine (TEA), various solvents, etc.) were obtained from commercial sources and used without further purification. Column chromatography was performed with Selecto Scientific Silica gel (particle size 100–200 μm). All reactions were monitored by thin-layer chromatography (TLC) using Merck silica gel plates 60 F₂₅₄; visualization was accomplished with UV light and/or staining with appropriate stains (iodine, vanillin). Reactions were monitored by gas chromatography-mass spectrometry (GC-MS, Electron Impact ionization, 70 eV) with a Shimadzu GCMS-QP2010S dual flow control and FID secondary detection and Shimadzu GC-2014 system 30 m and

15 m column length, respectively, and with an Agilent 6850 GC-5973 MS system (70 eV electron impact ionization) using a 30-m-long DB-5 type column (J&W Scientific).

Nuclear magnetic resonance spectroscopy Nuclear magnetic resonance (NMR) spectra were recorded on an Agilent MR400DD2 spectrometer, with a multinuclear probe with two RF channels and variable temperature capability. The measurements were carried out at 400 MHz-¹H NMR, 100 MHz-¹³C NMR, and 376 MHz-¹⁹F NMR. The solvents used that were purchased from Sigma-Aldrich include CDCl₃, benzene-*d*₆, diethyl ether-*d*₁₀, DMSO-*d*₆, and acetone-*d*₆. The NMR signals are reported in parts per million (ppm) relative to tetramethylsilane or the residual signal of the solvent.

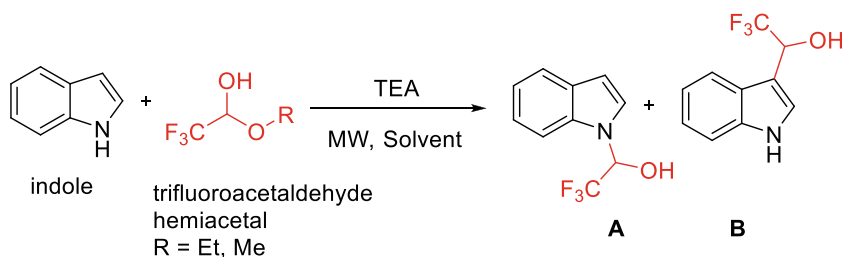
Typical reaction conditions Indole (0.05 g, 1 eq.), trifluoroacetaldehyde methyl hemiacetal (315 μL , 7 eq.), triethylamine (6.4 μL , 10 mol%), and the solvent (0.5 mL) were mixed together in a microwave vial (10 mL). This solution was irradiated in a closed vessel mode using a CEM-Discover microwave reactor at 80 °C. Aliquots were withdrawn for analysis at desired times. The completion of the reaction was monitored by TLC and GC-MS. Products were purified by flash chromatography.

Isolation of products obtained in non-polar and polar protic solvents: Upon completion of the reaction, the glass vessel was cooled down to room temperature and the mixture was extracted twice with diethyl ether. The ether layer was decanted and washed with water and saturated aqueous NaHCO₃. The organic layer was dried over MgSO₄, filtered, and the solvent was removed by a rotary evaporator. The product was purified by flash chromatography (silica gel, *n*-hexane/ethyl acetate, gradient 10–25% ethyl acetate).

Isolation of products obtained in polar aprotic solvents: The crude product was directly loaded on to silica column and was purified by flash chromatography using hexane/ethyl acetate gradient (10–20% ethyl acetate).

2,2-trifluoro-1-(1-*H*-indol-1-yl)ethanol (A): MS (EI) *m/z*: 117 (100%), 118 (85%), 215 (54%, M⁺), 146 (41%); ¹H NMR (400 MHz, (CD₃)₂CO): δ (ppm) 7.66 (d, *J* = 8.4 Hz, 1H), 7.58 (dt, *J* = 8.0, 1.2 Hz, 1H), 7.47 (d, *J* = 3.2 Hz, 1H), 7.16–7.22 (m, 1H), 7.06–7.12 (m, 1H), 6.55–6.59 (m, 1H), 4.04 (q, *J* = 6.8 Hz, 1H), 2.94 (br s, 1H); ¹³C NMR (101 MHz,

Scheme 1 Formation of indole-trifluoromethyl carbinols **A** and **B** from indole and trifluoroacetaldehyde hemiacetals in the presence of triethylamine (TEA)



(CD₃)₂CO): δ (ppm) 137.02, 130.01, 125.95, 124.3, 123.03, 121.72, 121.27, 111.34, 104.56, 77.03 (q, $J=36.3$ Hz); ¹⁹F NMR (376 MHz, (CD₃)₂CO): δ (ppm) -81.05 (d, $J=5.2$ Hz)
 2,2,2-trifluoro-1-(indol-3-yl)ethanol (**B**): MS (**EI**) m/z : 118 (100%), 146 (92%), 215 (48%, M⁺), 197 (11%); ¹H NMR (400 MHz, CDCl₃): δ (ppm) 8.3 (br s, 1H), 7.75 (d, $J=8.4$ Hz, 1H), 7.17–7.45 (m, 4H), 5.38 (q, $J=6.8$ Hz, 1H), 2.43 (br, 1H); ¹³C NMR (101 MHz, CDCl₃): δ (ppm) 136.01, 126.2, 125.68, 123.65, 123.63, 122.93, 120.59, 119.32, 111.40, 67.56 (q, $J=33.3$ Hz); ¹⁹F NMR (376 MHz, CDCl₃): δ (ppm) -77.91 (d, $J=6.8$ Hz)

Computational methods Geometry optimization of the reactant, product, and transition state structures have been carried out at B3LYP [31, 32]/6-31G(d,p) level of theory using Gaussian 09 suite [33]. Frequency calculations of all optimized structures were performed to confirm the minima and transition state structure with one imaginary frequency. The effect of solvent on overall reaction has been investigated implicitly as well as explicitly. For that, the implicit integral equation formalism polarizable continuum model (IEF-PCM) of solvation has been used and those solvents that are utilized in experiments were considered [34]. In addition, the temperature factor (80 °C) was incorporated so as to mimic the experiment. Intrinsic reaction coordinate (IRC) calculations were performed for transition state structures to confirm that it connects well to product and reactant on the potential energy surface. Zero-point-corrected activation energy, free energy of activation, and other thermodynamic parameters are estimated from implicit calculations. The explicit role of solvent in the reaction has further been studied, and for that, possible stable complexes of indole with the solvent (DMSO, Et₂O, acetone, and benzene) and catalyst TEA were formed. Relative stabilization energies and binding energies of the complexes were estimated. ¹H NMR chemical shifts were obtained for these complexes in order to compare with experimental data [35]. Moreover, electrostatic potential (ESP) fit charges were calculated to identify the potential nucleophilic center on indole. CYLview software was used to generate the images from optimized geometries [36].

Results and discussion

Experimental solvent studies

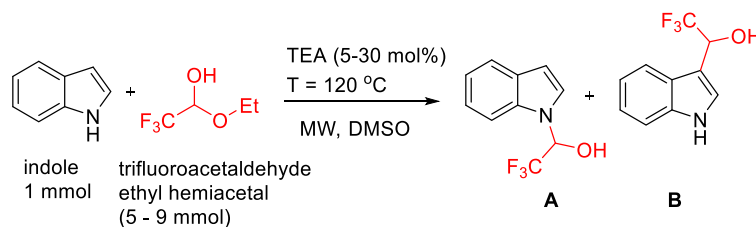
The effect of solvents on controlling the regioselectivity during the substitution of indoles has previously been studied but only in the presence of metal counter ions [21]. There are, however, many examples in the literature on the exquisite role of solvents in determining reaction rates [37] and selectivity [38]. The ability of solvents to control the outcome of a reaction depends on their capacity to coordinate with the reactants, intermediates, transition

states, or products. The reactant-solvent interaction is further dependent upon the type of solvent used and its polarity index [39] which can be categorized as non-polar, polar aprotic, or polar protic. Polar solvents can interact with electron-rich substrates and hence assist in specific bond cleavages [40] via solvation effects. Polar protic solvents due to their ability to participate in hydrogen bonding can help further activate and stabilize the intermediate. Non-polar solvents, however, only aid in solubilization of reactants and hence are not able to show any predominant solvation effects [28]. In the present work in addition to the experimental investigations, density functional theory (DFT) and NMR studies have been performed to better understand the driving forces of the solvent effect. Based on our previous works [8–13], the natural reactivity of indoles towards trifluoroalkylation lies at the C3 position (thermodynamically favored) under acidic conditions with microwave irradiation. The synthesis of N-substituted indole (kinetic control) is traditionally favored using strong bases or with metal-mediated reactions. However, as pointed out in our earlier work [8–13], the use of cinchona alkaloids, considered as strong organic bases, still resulted in the formation of the C3 product; thus, the base itself cannot ensure the selective formation of the N1-product. In contrast, as shown in our recent studies [15, 30], using polar aprotic solvents resulted in the exclusive formation of N-hydroxyalkylated indoles. The goal of the current study is to understand the fundamental basis of this exquisite solvent control on the regioselective outcome of the reaction by using different solvents ranging from non-polar to polar aprotic solvents in both experimental and theoretical investigations.

The trifluoroacetaldehyde alkyl (ethyl/methyl) hemiacetals and their hydrates are commercially available precursors for the in situ generation of trifluoroacetaldehyde (fluoral) via conventional or microwave heating [41] and consistent results (conversion or enantioselectivity) are observed using any alkyl hemiacetals [8–13, 42].

In order to observe the effect of solvents on the regioselective outcome of the reaction, all other reaction parameters were first optimized. The goal was to test the model reaction with sufficient conversion and high regioselectivity. The conditions were standardized with dimethyl sulfoxide (DMSO) as solvent.

The initial screening was carried out at 120 °C to determine the best molar ratio of the reactants and the amount of the base catalyst (triethylamine [TEA]) used, which was proposed to link to and partially deprotonate the slightly acidic N-H of indole to increase the electron density of the heterocyclic ring, thus increasing its reactivity. The results, tabulated in Table 1, show three different indole to trifluoroacetaldehyde ethylhemiacetal (TFAE) molar ratios (1:5, 1:7, 1:9) that were studied respectively (Table 1, entries 1, 3, and 5). Although use of nine equivalents of TFAE gave better percent conversion (78% in 15 min, Table 1, entry 5), the ratio of the N-substituted product was higher when 7 equivalent of TFAE was used (69% in 15 min, Table 1, entry 3) with no by-product

Table 1 Effect of reactant molar ratio and base concentration on the yield and selectivity of the microwave-assisted reaction of indole with trifluoroacetaldehyde ethyl hemiacetal in DMSO as a solvent

Entry	1/TFAE (TEA %)	Time (min)	Yield (%) ^a	Selectivity (%) ^b		Others (%) ^b
				A	B	
1	1:5 (10)	15	39	65	35	0
		30	77	46	42	12
2	1:7 (5)	15	57	59	36	5
		30	68	46	44	10
3	1:7 (10)	15	62	69	31	0
		30	73	44	37	19
4	1:7 (30)	15	67	50	37	13
		30	80	24	45	31
5	1:9 (10)	15	78	37	50	13
		30	92	20	50	30

Reagents and conditions: indole (1 mmol); trifluoroacetaldehyde ethyl hemiacetal (5–9 mmol); triethylamine (5–30 mol%); DMSO as solvent; $T = 120\text{ }^\circ\text{C}$, $P_{\text{max}} = 300\text{ W}$, with continuous stirring

^a GC yields, based on indole

^b Selectivity as determined by GC-MS

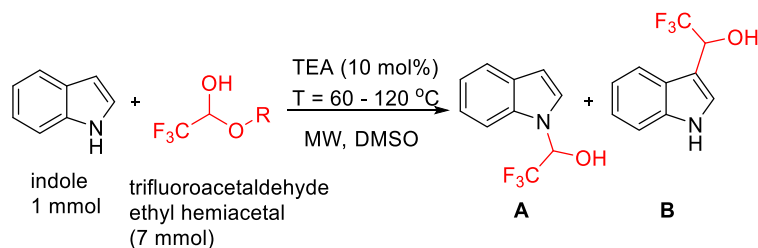
formation. Lower than 7 equivalents of TFAE gave low conversion (39% in 15 min; Table 1, entry 1). After the optimum indole:TFAE ratio was determined, the amount of base catalyst was standardized. Three different concentrations (5, 10, and 30 mol%) of base were tested (Table 1, entries 2, 3, and 4 respectively). After the screening, 10 mol% base concentration was selected for future reactions as it provided optimum conversion and selectivity.

Further studies were directed towards optimizing the reaction time and temperature. The data are summarized in Table 2. As shown, four different reaction temperatures (60 °C, 80 °C, 100 °C, and 120 °C) and six different reaction times (5, 10, 15, 20, 25, 30 min) were studied. As the temperature increases from 80 to 120 °C (Table 2, entries 2 and 4 for

15 min), the conversion of the reaction increases (from 18 to 62%) but the selectivity drastically decreases (from 92 to 69%).

Based on the selectivity of the product and maximum conversion of the reactant (indole) to its corresponding substituted derivative, the reaction temperature of 80 °C was selected. For the same reason, 30-min reaction time was determined to be best for further solvent-dependent studies. Reactions were also carried at 140 °C (data not included); however, these conditions yielded multiple by-products with no desired selectivity.

After the reaction conditions were standardized, the effect of a broad range of solvents was investigated on the yield and selectivity of the indole-carbinol products (Table 3). The list

Table 2 Effect of reaction temperature and time on the yield and selectivity of the microwave-assisted reaction of indole with trifluoroacetaldehyde ethyl hemiacetal in DMSO as a solvent

Entry	Temp (°C)	Time (min)	Yield (%) ^b	Selectivity (%) ^c		Others (%) ^c
				A	B	
1	60	15	4	99	1	0
		30	6	99	1	0
2	80 ^a	5	9	99	1	0
		10	16	93	7	0
		15	18	92	8	0
		20	22	94	6	0
		25	23	95	5	0
		30	25	93	7	0
3	100	15	36	88	12	0
		30	43	83	17	0
4	120	15	62	69	31	0
		30	73	44	37	19

Reagents and conditions: indole (1 mmol); trifluoroacetaldehyde ethyl hemiacetal (7 mmol); triethylamine (10 mol%); DMSO as solvent; $T = 60$ – $120\text{ }^\circ\text{C}$, $P_{\text{max}} = 300\text{ W}$, with continuous stirring

^a Time interval = from 5 to 30 min (microwave irradiation)

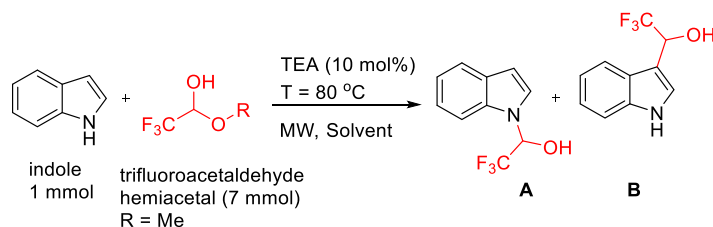
^b Determined by GC-MS, based on indole

^c Selectivity as determined by GC-MS

included a broad range of common solvents, from non-polar solvents such as hexane with polarity index of 0 and dielectric constant of $\epsilon = 1.89$ to DMSO with the highest polarity index of 7.2 and dielectric constant of $\epsilon = 46.45$. All reactions were carried out under identical experimental conditions except the solvent used.

The study showed direct relation between the polarity index/dielectric constant of the chosen solvents and its effect in controlling the regio/chemoselective outcome of the reaction. Based on the results (Table 3), solvents can be classified

under three main categories according to their behavior: (a) solvents leading to high conversion and high C-selectivity (hexane, toluene, CCl_4 , CHCl_3 , and CH_2Cl_2): where the selectivity of the reaction is completely directed towards the formation of C3-substituted product **B** (ranging from 98 to 90% respectively); (b) solvents leading to low conversion and high C-selectivity (diethyl ether, THF, ethyl acetate, ethanol, and acetone): in which selectivity of the reaction gradually shifting from C3 to N1-substituted product reaching nearly 1:1 ratio in acetone, although with low yield (20–40%); and

Table 3 Effect of solvent polarity on the yield and selectivity of the microwave-assisted reaction of indole with trifluoroacetaldehyde methyl hemiacetal

entry	solvent	P ^a	ϵ^b	Yield (%) ^c	Selectivity (%) ^d		Others (%) ^d
					A	B	
1	hexane	0	1.89	100	0	98	2
2	CCl ₄	1.6	2.24	98	1	93	6
3	toluene	2.4	2.38	98	1	92	7
4	Et ₂ O	2.8	4.20	49	8	87	5
5	CH ₂ Cl ₂	3.1	8.93	99	1	90	9
6	CHCl ₃	4.1	4.89	99	1	93	6
7	THF	4.2	7.58	31	16	80	4
8	EtOAc	4.4	6.02	28	14	84	2
9	EtOH	5.2	24.55	24	13	87	0
9	acetone	5.4	20.70	38	47	53	0
10	CH ₃ CN	5.8	35.94	64	67	29	4
11	DMF	6.4	36.71	51	94	5	1
12	DMSO	7.2	46.45	44	91	0	9

Reagents and conditions: indole (1 mmol); trifluoroacetaldehyde methyl hemiacetal (7 mmol); triethylamine (10 mol%); T = 80 °C, P_{max} = 200 W, with continuous stirring

P polarity index, ϵ dielectric constant

^a Solvent miscibility chart is downloaded from <http://phx.phenomenex.com/lib/gu54810610.pdf>

^b Dielectric constant (relative permittivity) of the pure liquid is measured at 25 °C [28]

^c Determined by GC-MS, based on indole

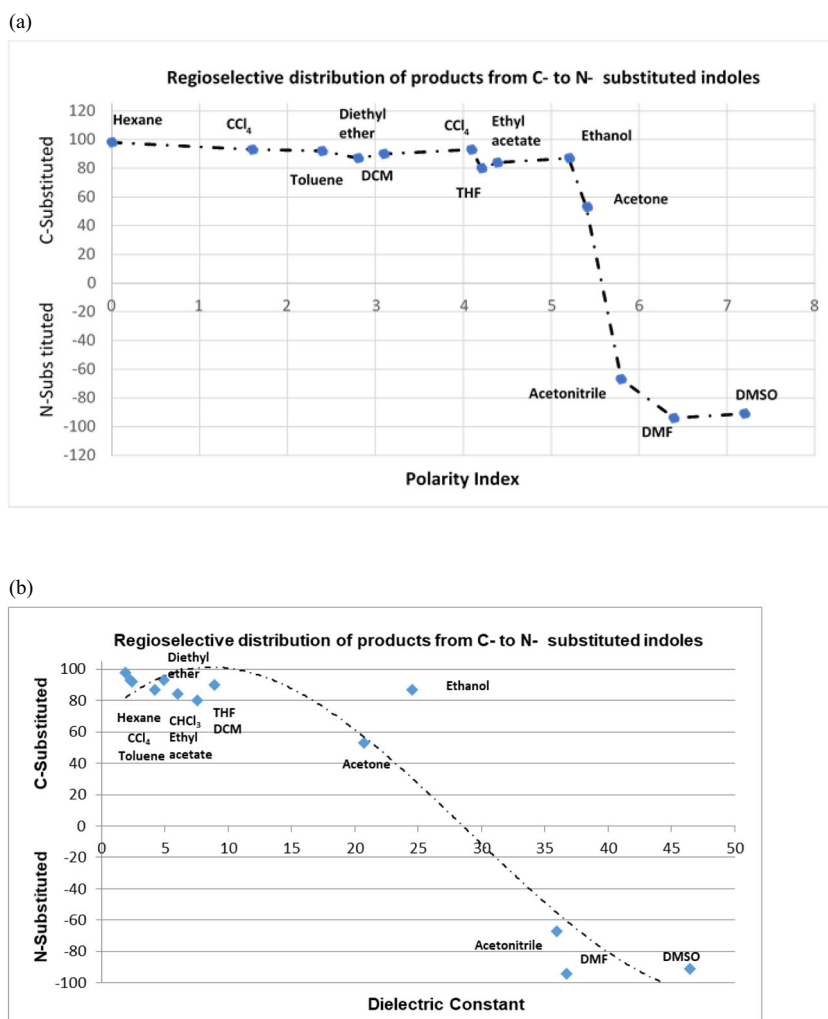
^d Selectivity as determined by GC-MS

(c) solvents leading to moderate conversion and high N-selectivity (acetonitrile, DMSO, and DMF). The reaction carried out in DMSO favors the formation of N-substituted product **A** with almost 100% selectivity representing a major shift in N1-selectivity. Figure 1 given below shows the selectivity distribution of C- and N-substituted products as a function of the polarity of the solvent (a) and dielectric constant (b). The

formation of C-substituted product, which is dominant in non-polar and polar protic solvents, further diminishes when polar aprotic solvents were used and leads to product with N-selectivity.

The experimental data obtained in the TEA-catalyzed reactions prompted us to investigate the role of the catalyst. Three solvents from the three major parts of the regioselectivity vs.

Fig. 1 Effect of the solvent polarity (a) and dielectric constant (b) on the regioselectivity of C- to N-product formation in the microwave-assisted reaction of indole with trifluoroacetaldehyde methyl hemiacetal

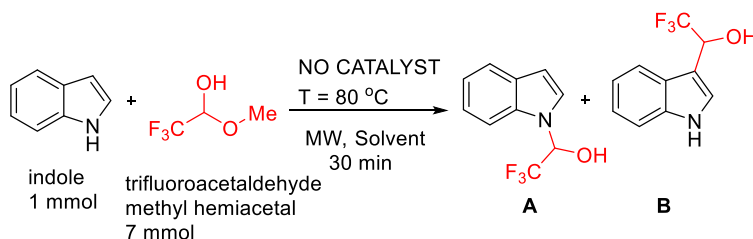


polarity functions have been chosen for the investigation. These solvents were hexane (exclusive C3-selectivity), acetone (~1:1 ratio of C/N products), and DMSO (exclusive N-selectivity). The data are tabulated in Table 4.

From Table 4, it has been observed that the reaction readily occurs in the solvents without the presence of the catalyst. In hexane, neither the yield nor the C3-selectivity appears to be affected (Table 4, entry 1). In DMSO, the reaction rate drops to half of that of the catalyzed reaction; however, the reaction results in exclusive N-selectivity (Table 4, entry 3). Surprisingly, acetone that had produced a 1:1 ratio of **A** and **B** with TEA yielded 100% C3 product (**B**) albeit with lower reaction rate. In conclusion, while the catalyst aids the reaction rate and affects the regioselectivity in case of midrange polarity, the selectivity appears to be exclusively determined by the solvent at the non-polar and highly polar end of the solvent spectrum. In addition to its role as a catalyst, it also can act as a co-solvent. Its dielectric constant ($\epsilon = 2.4$) is similar to that of toluene, and it can shift the selectivity towards the formation of the C3-substituted product **B**, thus explaining that without TEA, the **A** selectivity in DMSO improved to 100% (Table 4, entry 3).

Density functional theory and NMR studies

Based on the above data, it is unambiguous that the solvent has a decisive contribution to determine the regioselectivity of the reaction. Moreover, it is also clear that the presence of the catalyst is not necessary to obtain exclusive selectivity for either of the products. These primary observations regarding the solvent effect led us to carry out theoretical studies. To obtain the relative thermodynamic stability of the products, density functional theory (DFT) calculations have been carried out at the B3LYP/6-31G(d,p) level of theory. Optimized geometries and relative stabilization energies of the products in the gas phase and in the different solvents are shown in Fig. 2. The data show that the C3-substituted product (**B**) is thermodynamically more stable than the N-substituted product (**A**) in the gas phase and in each targeted solvent. However, the respective stabilization energy differences change in implicit solvent studies. The 5.5 kcal/mol difference almost doubled to 9.8 kcal/mol when the compounds were calculated in benzene. This energy difference decreases to 6.8 kcal/mol in ethanol or acetonitrile. When DMSO was applied as a solvent, a significant further decrease was observed to

Table 4 Effect of solvent polarity on the yield and selectivity of the microwave-assisted reaction of indole with trifluoroacetaldehyde methyl hemiacetal in a catalyst-free medium

entry	solvent	P	ϵ	Yield (%) ^b	Selectivity (%) ^c		Others (%) ^c
					A	B	
1	hexane	0	1.89	100	0	100	0
2	acetone	5.4	20.70	22	0	100	0
3	DMSO	7.2	46.45	21	100	0	0

Reagents and conditions: indole (1 mmol); trifluoroacetaldehyde methyl hemiacetal (7 mmol); T = 80 °C, P_{\max} = 200 W, with continuous stirring
P polarity index, ϵ dielectric constant

^a GC yields, based on indole

^b Selectivity as determined by GC-MS

3.2 kcal/mol. The relative stabilization energy data indicate that while the solvents profoundly affect the thermodynamic stability of the products, the C3 product is still more stable. Thus, while the energies support the shift in selectivity, the opposite selectivities in different solvents cannot be explained as an exclusive result of thermodynamic stability.

As a next step, the implicit role of solvent has been investigated employing IEF-PCM model of solvation. The reaction of indole with trifluoroacetaldehyde methyl/ethyl hemiacetal is considered at 80 °C with wide range of implicit solvents.

Calculations carried out in DMSO are used as representative model in the figures as shown in Fig. 3.

Trifluoroacetaldehyde methyl/ethyl hemiacetal (TFA) can interact in two different geometries (*re* and *si* face) that would produce different enantiomeric hydroxyalkylated products and lead to four isomeric products, namely **Ind_TFAA_A_R** and **Ind_TFAA_A_S** (product A is N1-substituted), and **Ind_TFAA_B_R** and **Ind_TFAA_B_S** (product B is C3-substituted). Possible stable complexes of indole interacting with TFA in both directions were generated in which indole N-H

Fig. 2 Optimized geometry and relative stabilization energy of C- to N-substituted indolyl-trifluoromethyl ethanols at B3LYP/6-31G(d,p) level. Electronic energy E is in hartrees and relative stabilization energies (ΔE_{rel}) are in kcal/mol

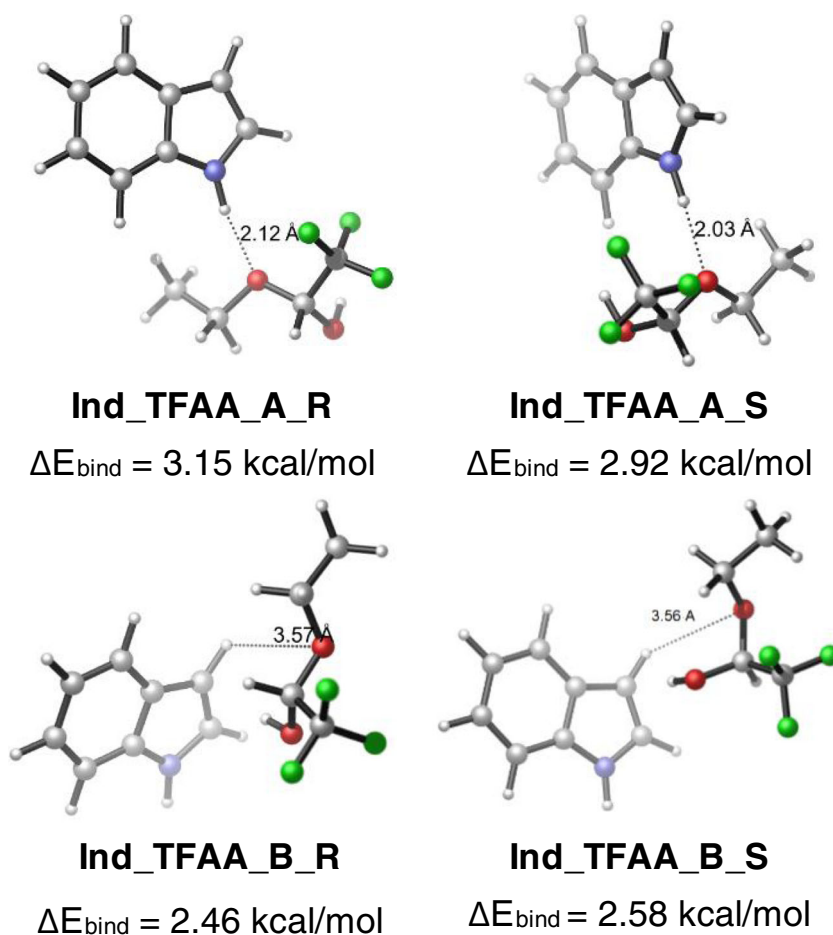


Product A ($E = -815.220471$)
 $\Delta E_{rel} = 5.5$ kcal/mol (gas)
 $\Delta E_{rel} = 9.8$ kcal/mol (benzene)
 $\Delta E_{rel} = 6.8$ kcal/mol (AcCN)
 $\Delta E_{rel} = 6.8$ kcal/mol (EtOH)
 $\Delta E_{rel} = 3.2$ (DMSO)



Product B ($E = -815.229251$)
 $\Delta E_{rel} = (0.0)$

Fig. 3 IEF-PCM optimized geometries of indole interacting with trifluoroacetaldehyde ethyl hemiacetal. Binding energies (ΔE_{bind}) are given in kcal/mol. A and B refer to the N- and C-products while R and S indicate the potential chirality the interaction would lead to



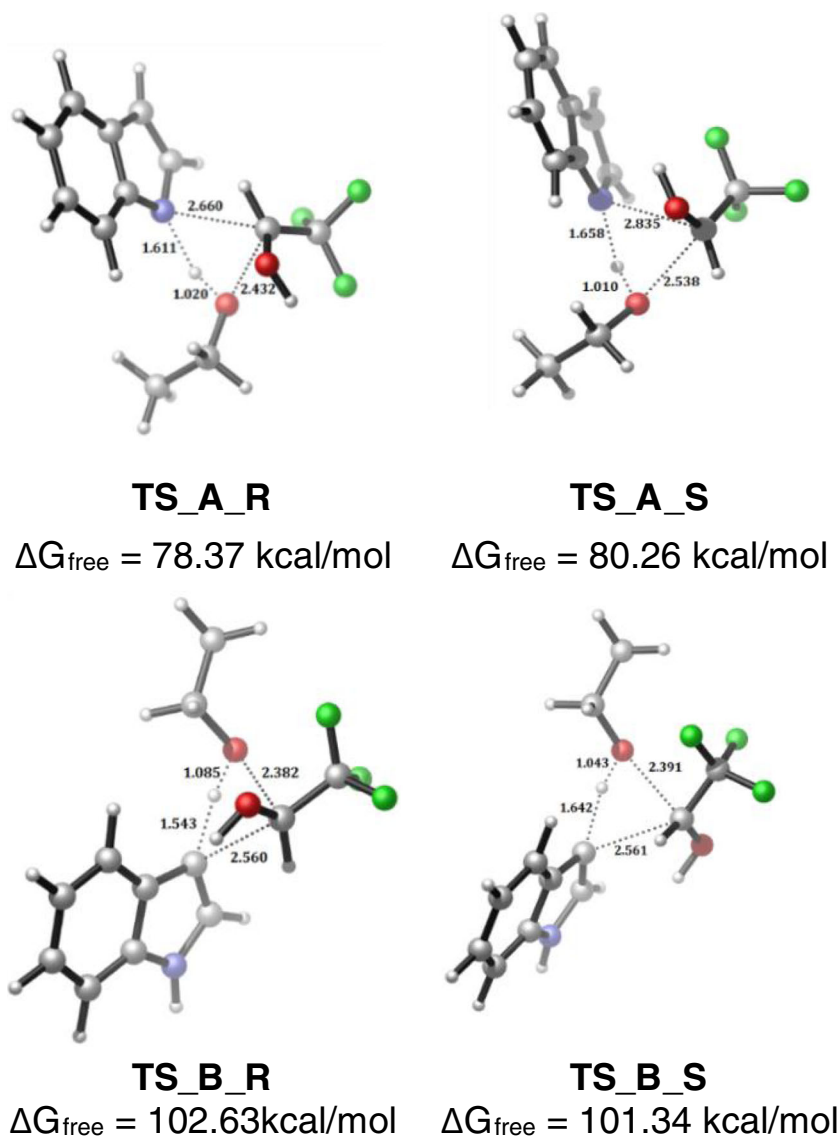
and C-H are alternately interacting with ethoxy oxygen of TFAA (Fig. 3). The optimized geometries obtained in DMSO as a solvent are shown in Fig. 3 along with interaction energies in kcal/mol. The optimization reveals the lowest energy complex is with the interaction between indole N1-H and ethoxy oxygen (N-H \cdots O \sim 2.12 Å). The calculated binding energy is around 3.15 kcal/mol (**Ind_TFAA_A_R**). On the other hand, the bond distance in the C3-H \cdots O interaction of indole and TFAA are longer (3.56 Å) and comparatively destabilized with 2.46 kcal/mol of binding energy (**Ind_TFAA_B_R**). It has been observed that the binding energy differences between the isomeric R and S complexes are only 0.23 kcal/mol for **A**(R/S) products and 0.12 kcal/mol for **B**(R/S) products.

Furthermore, the transition states for each of these complexes were located in order to find the favorable path of the reaction (Fig. 4).

Optimization of transition state is carried out in a wide range of solvents. Transition state geometries obtained for complexes **Ind_TFAA_A_R** and **S** (abbreviated as **TS_A_R** and **S**) and **Ind_TFAA_B_R** and **S** (abbreviated as **TS_B_R** and **S**) in DMSO are shown in Fig. 4 along with activation-free energies

in kcal/mol. The calculations show that the lowest energy transition state is **TS_A_R** which leads to N1-substituted product **A** with activation-free energy of 78.37 kcal/mol, whereas transition state for C3-substituted products **TS_B_S** and **TS_B_R** appear destabilized in DMSO by 22.97 and 24.26 kcal/mol, respectively, compared to that of **TS_A_R** or **TS_A_S**. Transition state geometries show that the distance between N \cdots C and C \cdots O is relatively short in **TS_A_R** compared to that found in **TS_A_S** which further reflects in their activation-free energy difference by 1.89 kcal/mol. However, in **TS_B_S** and **TS_B_R** structures, these interactions show considerably lower difference and merely differ in their energies by 1.29 kcal/mol. Calculated zero-point-corrected activation energy, activation-free energy, and other thermodynamic parameters such as change in enthalpy, entropy, and internal energies are given in Table S1 for trifluoroacetaldehyde ethyl hemiacetal (TFAA). It has been observed that ethanol and DMSO show lower activation-free energy for **TS_A_R** path. The energy trend for activation-free energy in different solvents is as follows (data given in kcal/mol): EtOH (77.73) < DMSO (78.37) < THF (78.55) < CH₃CN (78.56) < CH₂Cl₂ (78.70) < acetone (78.95) < CHCl₃ (79.42) < Et₂O

Fig. 4 IEF-PCM derived geometries of transition state at B3LYP/6-31G(d,p)** level of theory for **TS_A_(R/S)** and **TS_B_(R/S)**. Activation-free energy (ΔG_{free}) is given in kcal/mol

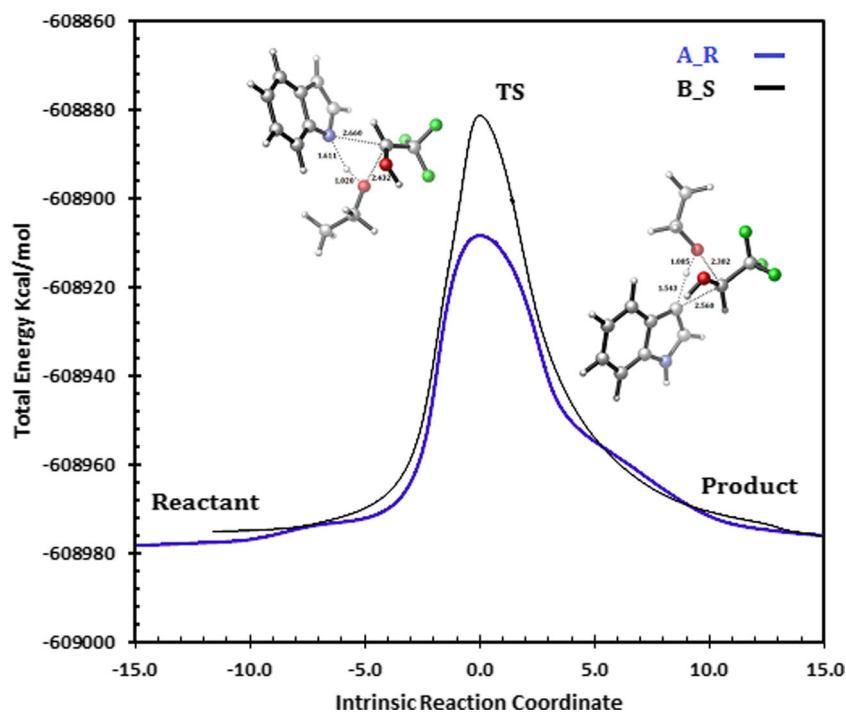


(79.43) < hexane (79.70) < toluene (79.89) < CCl_4 (80.12) < DMF (90.41). Similarly, calculations for trifluoroacetaldehyde methyl hemiacetal (TFAA-Me) were also carried out in selected solvents such as DMSO, acetone, and hexane. The data is shown in Table S1. In addition, the transition state geometries and energies for the indole-TFAA-Me complexes have been calculated and are depicted in Fig. S1. It was observed that, as expected, the change of the ethyl group to methyl did not affect the transition state stabilities significantly. The obtained free energies followed the same trend as in Fig. 4, the change in the actual kcal/mol values was within 1%.

Intrinsic reaction coordinate (IRC) calculations for each transition state were performed in order to verify the smooth reaction path connecting well with reactant and product on the potential energy surface. Figure 5 shows the IRC plot for the lowest energy N-substituted (**A_R**) and destabilized C-substituted (**B_S**) path of the reaction.

As shown in Fig. 5, the implicit calculations in DMSO unambiguously favor the path which leads to N1-substituted product. Similarly, the calculated internal energy values (ΔU in Table S1) also offer a clear explanation to the experimentally observed C3-selectivity in other solvents as well. The internal energy data show an inverse relationship for the N1- and C3-product leading transition states, the total energies for N1 transition states are significantly lower in DMSO than in hexane, while for C3 the opposite was found, in agreement with the experimental findings. However, since implicit calculations do not always sufficiently represent the individual interactions between the solvent and substrates, it was decided to investigate the explicit interaction of indole with solvents and the catalyst triethyl amine (TEA) as well. In these calculations, dimethyl sulfoxide (DMSO), diethyl ether, acetone, and benzene are used as model solvents. Figure 6 displays various optimized complexes of indole with the catalyst and

Fig. 5 Calculated intrinsic reaction coordinate (IRC) at B3LYP/6-31G(d,p) level of theory employing IEF-PCM (DMSO) model of solvation for transition states **TS_A_R** and **TS_B_S**



the solvent molecules, respectively. The proposed active sites which participate in the hydrogen bonding interaction in indole is N1–H and C3–H [43]. In case of DMSO, both the O- and S-atoms were separately considered as H-bond acceptors while in the other solvents, with the exception of benzene, the singular heteroatom fulfilled this role. The data indicate that while TEA, DMSO, Et₂O, and acetone were able to form individual complexes with indole on its N1–H and C3–H positions, benzene formed a nondescript complex. The calculated relative stabilization and binding energy data reveal that the lowest energy complex is where indole N–H is interacting with heteroatom of the solvent or the catalyst. The stability of these complexes can be attributed to the stronger acidity of the N–H bond compared to that of the C3–H, which accordingly forms a stronger hydrogen bond with H-bond acceptors. Accordingly, the N–H···O and N–H···N bonds show shorter interaction length than that of the respective C–H···O and C–H···N bonds of the less stable complexes. It is interesting to note that the Ind-N-DMSO complex has binding energy of 10.34 kcal/mol which is comparatively larger than that of Ind-N-TEA complex (7.88 kcal/mol). Despite the stronger basicity of TEA, indole shows larger binding affinity towards DMSO. When calculation of an indole-benzene stacking conformer was attempted, it did not converge. Similarly to the optimized geometries of potential complexes with chloroform are void of any interactions (Fig. S3) indicating relatively weak interaction between non-polar solvent and indole.

These findings, when considered with the thermodynamic stability of the products in different solvents (Fig. 2), suggest that the low polarity solvents do not change the traditional Friedel-Crafts mechanism leading to

product **B** and the product distribution is likely determined by the thermodynamics of the products in those solvents.

Furthermore, a simultaneous interaction of indole with catalyst TEA and DMSO has also been investigated, where indole N–H and C3–H consecutively interacting with TEA and DMSO (**Ind-TEA-DMSO-1** and **Ind-TEA-DMSO-2**). Optimized geometries of these complexes are shown in Fig. 7 along with their relative stabilization and binding energies.

The relative stabilization and interaction energy data show that the difference between the two isomers are relatively insignificant; however, DMSO appear to form stronger bonding interaction with indole in either positions as evident from the shorter bond lengths.

In addition to optimization of the above complexes, several other properties such as ¹H NMR chemical shifts (Table 5) as well as electrostatic potential (ESP) fit charges for these complexes (Table 6) have been calculated. As TFAA is an electrophile, it is suggested that the more nucleophilic center will likely serve as potential reactive site for substitution in indole. A comparison of the calculated chemical shifts with experimental NMR data may help in experimentally confirming the presence of dominant species. Also the ESP fit charges of complexes aid in identifying the reactive center in indole.

It has been observed that ¹H NMR chemical shifts derived from the explicit interaction of indole N–H and DMSO (**Ind-N-DMSO**)[N–H(10.6); C2–H(7.0); C3–H(6.4)] are in good agreement with experimental data of **Ind-DMSO-d₆** [N–H(11.1); C2–H(7.0); C3–H(6.4)]. In contrast, explicit **Ind-**

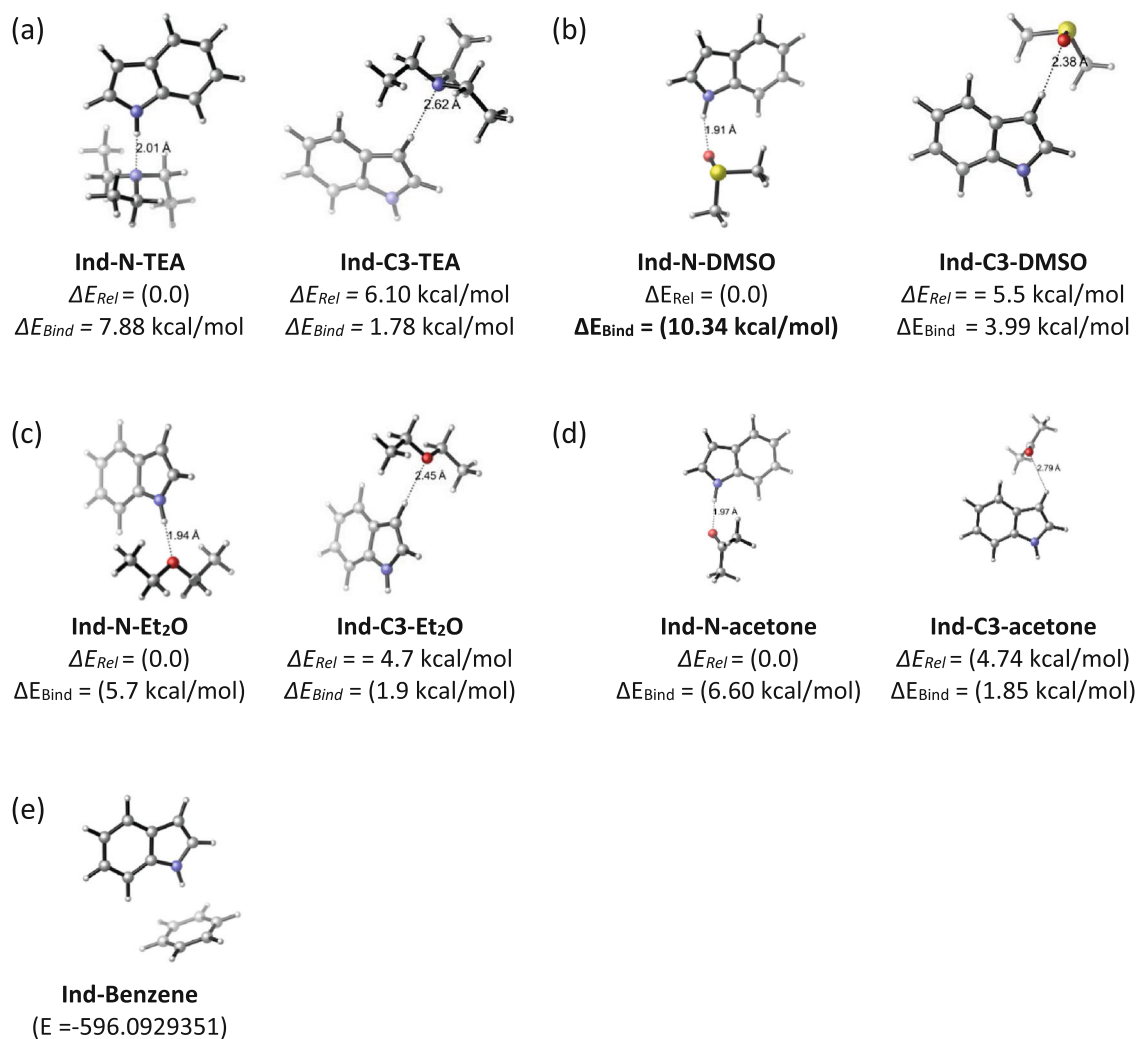


Fig. 6 Optimized geometries of indole interacting with **a** triethylamine, **b** dimethyl sulfoxide, **c** diethyl ether, and **d** acetone and **e** benzene at the B3LYP/6-31G(d,p) level

C3-H-DMSO chemical shift data are not a good match with the experimental values. Similar conclusions can be drawn from the **Indole-Et₂O** ¹H NMR data. As the ¹H NMR chemical shifts are influenced by the presence of

electron density cloud around the proton, the up- or downfield shifts reflected in the spectra help to identify the possible complexes. Comparison with the theoretically calculated values further validate the proposed binding mode. The data in Table 5 clearly support that the dominant solvated form has N–H···X (X = O,N) interactions. Interestingly, the addition of **TEA** to **Ind-DMSO** did not result in any spectral change. The data show better agreement with the calculated N–H and C2–H proton chemical shifts of **Ind-TEA-DMSO-2** complex than that of **Ind-TEA-DMSO-1** (Table 5, entries 16 and 17). Thus, **Ind-TEA-DMSO-2** appears to be the more probable complex based on the NMR studies.

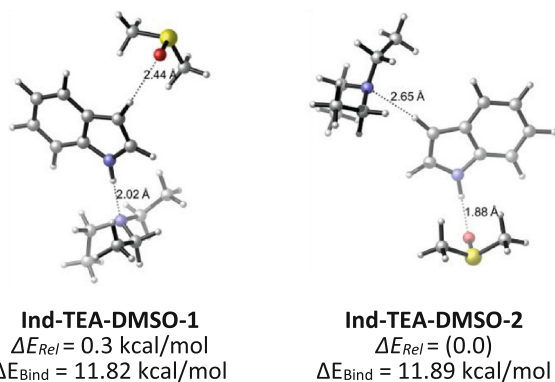


Fig. 7 Simultaneous interaction of indole with TEA and DMSO optimized at the B3LYP/6-31G(d,p) level

The ESP fit charges calculated for these complexes (Table 6) show that the interaction of indole with solvents has a profound effect on the electron density of the reactive N1 and C3 atoms of indole.

Ind-N-TEA and **Ind-N-Et₂O** complexes show depletion of negative charge on the N1 atom that is involved

Table 5 Calculated and experimental (Exp) ^1H NMR chemical shifts for selected positions of indole

Entry	Complex	^1H -NMR chemical shift (in ppm)		
		N-H	C2-H	C3-H
1	Ind (gas phase)	7.1	7.0	6.5
2	Ind-benzene (implicit)	7.5	7.1	6.5
3	Ind-DMSO (implicit)	7.9	7.3	6.6
4	Ind-benzene-d_6 Exp	6.6	6.5	6.4
5	Ind-TEA (benzene-d_6) Exp	8.7	6.8	6.5
6	Ind-DMSO-d_6 Exp	11.1	7.0	6.4
7	Ind-TEA-DMSO-d_6 Exp	11.1	7.0	6.4
8	Ind-Et$_2$O-d_{10} Exp	9.8	6.9	6.4
9	Ind-N-TEA	11.4	7.0	6.5
10	Ind-C3-TEA	7.1	7.0	7.8
11	Ind-N-DMSO	10.6	7.0	6.4
12	Ind-C3-DMSO	7.2	7.1	8.1
13	Ind-N-Et$_2$O	9.9	6.9	6.4
14	Ind-C3-Et$_2$O	7.1	7.0	7.5
15	Ind-benzene	5.1	6.6	6.3
16	Ind-TEA-DMSO-1	11.4	7.2	7.9
17	Ind-TEA-DMSO-2	11.0	7.0	7.7

in the interaction while the C3 atom increases the nucleophilicity. However, in **Ind-N-DMSO** and **Ind-TEA-DMSO-2** complexes, enhanced negative charge on N1 atom is evident which may play a significant role in directing the electrophile towards the nitrogen of indole in DMSO solution.

Table 6 Calculated electrostatic potential (ESP) fit charges for selected positions of indole

Entry	Complex	ESP charges		
		N	C2	C3
1	Ind (gas phase)	-0.44303	-0.00949	-0.35601
2	Ind-N-TEA	-0.21667	-0.01328	-0.38545
3	Ind-C3-TEA	-0.43101	-0.03103	-0.30347
4	Ind-N-DMSO	-0.37311	-0.00617	-0.35244
5	Ind-C3-DMSO	-0.42708	-0.02823	-0.24909
6	Ind-N-Et$_2$O	-0.37023	-0.00144	-0.38849
7	Ind-C3-Et$_2$O	-0.40484	-0.02564	-0.32999
8	Ind-N-acetone	-0.44592	0.01622	-0.36034
9	Ind-C3-acetone	-0.42852	0.00085	-0.33859
10	Ind-benzene	-0.48009	0.03208	-0.33508
11	Ind-TEA-DMSO-1	-0.24386	-0.04221	-0.30322
12	Ind-TEA-DMSO-2	-0.37866	-0.05418	-0.27935

Explicit solvent studies show that the interaction of indole with the solvent significantly changes the electrostatic charges on the atoms of interest (N1 and C3) which may contribute to the underlying driving force of chemo/regioselectivity. Since the experimental data (Table 3) clearly showed that the catalyst (**TEA**) is not necessary for the reaction to occur in either solvent and produce exclusive N1-selectivity in DMSO, the further computational studies were focused on DMSO only.

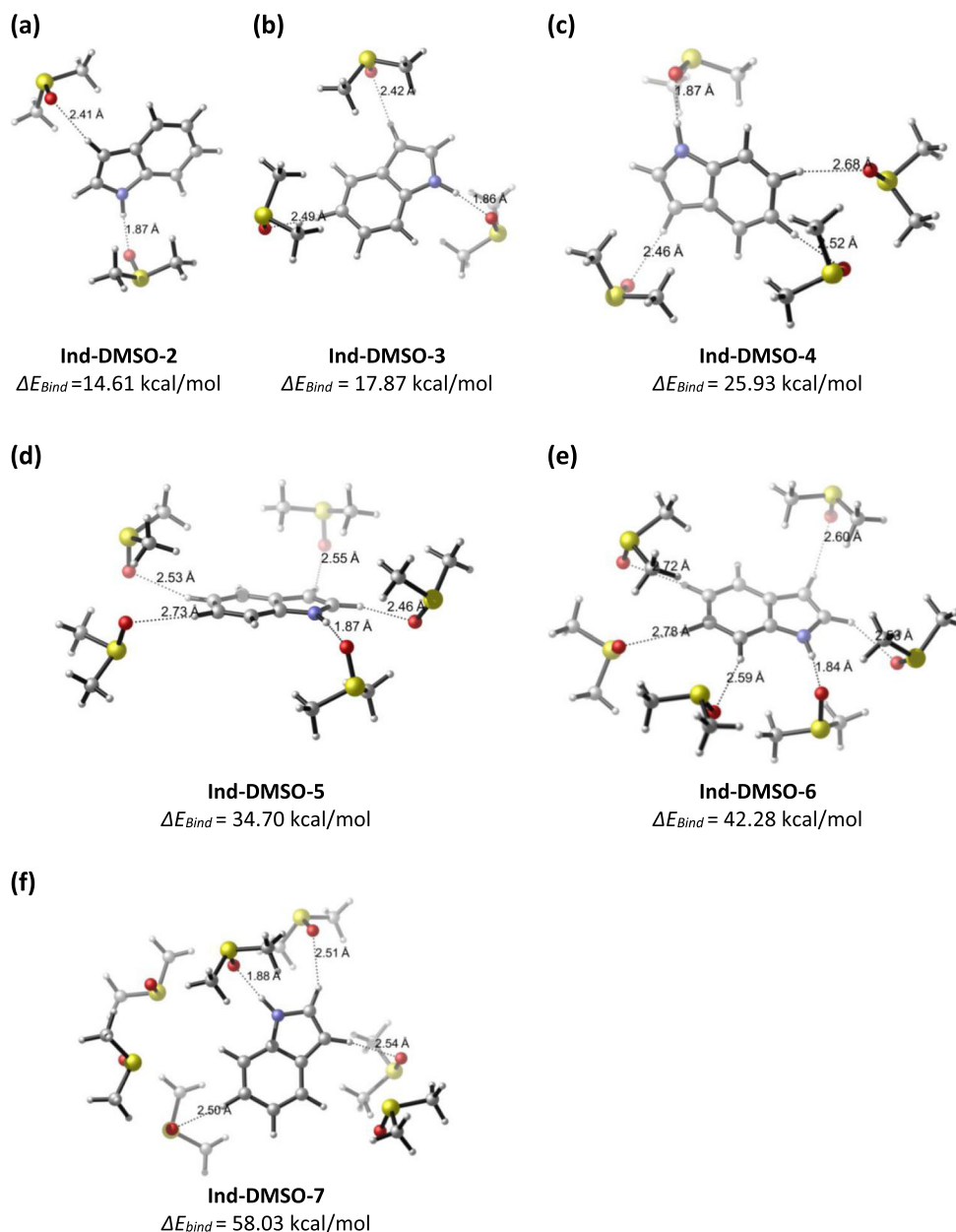
The calculations related to the equimolar indole-DMSO complex describe how location of interaction influences the ESP charges on atoms of interest. In actual experiments, the indole to DMSO molar ratio is much higher and to study the realistic model of explicit interaction, more DMSO molecules were incorporated successively in the calculations. This provides more insight into the potential nature of the DMSO solvated indole. Optimized geometries of indole-DMSO complexes with increasing stoichiometric ratio are shown in Fig. 8 along with binding energies in kcal/mol.

The ^1H NMR chemical shift and ESP fit charges for these complexes are tabulated in Tables 7 and 8. Calculated shifts for these complexes may reveal the size of the potential solvation sphere around indole when compared with experiment. Likewise, ESP charges could explain the directing effect of DMSO.

The optimized geometries show that indole is able to make reasonably stable complexes with DMSO up to a 1:4 ratio where all four DMSO molecules are interacting with indole. When more than five or six solvent molecules are brought into contact with indole, then few DMSO loses the interaction with indole. Once all seven hydrogen of indole are targeted in interactions with DMSO, the complex diverged and resulted in the formation of a complex with 1:4 stoichiometry and three spectator DMSO units. These observations indicate that complexes with more than 1:4 stoichiometry are unlikely to play a role in the reaction. The analysis of the ESP charges of the 1:4 and smaller complexes reveal that the dominant nucleophile in the indole structure is the N-atom; however, in later complexes, depletion of negative charge on nitrogen atom is evident.

The calculated ^1H -NMR data show varied correlation to the experimental chemical shifts. Considering the chemical shift values of C3-H, 1:1 complex represents the perfect fit (Table 7, entry 1), while the N-H shift is only drifted off by 0.5 ppm. Although the higher indole to DMSO complexes show better correlation to the N-H chemical shift, both calculated C-H values are significantly ($\Delta\delta_{\text{H}} \sim 1.5$ ppm) higher than the experimentally observed shift. This suggests that once the 1:1 complex forms on the N-H bond of indole, the other DMSO molecules can rather be seen as spectators and do not

Fig. 8 a–f Interaction of indole with dimethyl sulfoxide in different stoichiometry optimized at the B3LYP/6-31G(d,p) level



appear to engage in a formal hydrogen bonding interaction with the C3–H of indole.

Conclusions

Solvent polarity appears to have a crucial effect on the regio/chemoselectivity of the hydroxyalkylation of indole with trifluoromethylacetaldehyde hemiacetals. After careful experimental optimization, it was observed that the reaction produced the expected C3-hydroxyalkylated product in nearly 100% selectivity in non-polar solvents; however, it dramatically shifted towards the exclusive

formation of the N1-substituted product in highly polar aprotic solvents. In order to establish a reasonable proposed mechanism for the profound selectivity shift, extended experimental and theoretical investigations were carried out. A gradual shift in selectivity was observed from the C3 to N1 product formation as a function of solvent polarity in experimental studies. It has also been established via experiments that the reactions, while with lower rate, readily occurred in both solvent types producing the same selectivity without a catalyst. Thus, the catalyst results in rate enhancement; however, its role in determining selectivity is insignificant. Theoretical DFT calculations as well as NMR investigations revealed that the

Table 7 Calculated and experimental (exp) ^1H NMR chemical shifts for selected positions of indole in DMSO

Entry	Complex	^1H -NMR chemical shift (ppm)		
		N-H	C2-H	C3-H
1	Ind-N-DMSO	10.6	7.0	6.4
2	Ind-C3-DMSO	7.2	7.1	8.1
3	Ind-DMSO-2	11.2	7.2	8.0
4	Ind-DMSO-3	11.3	7.2	8.0
5	Ind-DMSO-4	11.1	7.2	7.9
6	Ind-DMSO-5	11.1	8.2	7.6
7	Ind-DMSO-6	11.7	8.1	7.5
8	Ind-DMSO-7	11.2	8.1	7.7
9	Ind-DMSO (implicit)	7.9	7.3	6.6
10	Ind-DMSO- d_6 (exp)	11.1	7.0	6.4

interaction of non-polar solvents with indole is negligible. Therefore, it is proposed that the significantly higher thermodynamic stability of the C3-hydroxyalkylated product determines the outcome of the reaction in non-polar and low polarity solvents. The calculations, however, revealed significant interaction between polar aprotic solvents and indole. Specifically, the potential hydrogen bonding between the solvents and N1-H and C3-H was studied. The results confirmed that the interaction of DMSO with indole created an electronic environment where the nucleophilicity of the N1 is significantly higher than that of the C3, effectively attracting the attacking electrophile to N1, thus ensuring the exclusive selectivity for the N1-hydroxyalkylated product. According to the calculations, the 1:1 indole-DMSO complex appears to be the most likely species to be responsible for the N- selectivity. This observation was supported by ^1H NMR experiments as well.

Table 8 Calculated electrostatic potential (ESP) fit charges for selected positions of indole in indole-DMSO complexes

Entry	Complex	ESP charges		
		N	C2	C3
1	Ind (gas phase)	-0.44303	0.00949	-0.35601
2	Ind-N-DMSO	-0.37311	-0.00617	-0.35244
3	Ind-C3-DMSO	-0.42708	-0.02823	-0.24909
4	Ind-DMSO-2	-0.40263	-0.00131	-0.31187
5	Ind-DMSO-3	-0.38996	-0.02247	-0.26781
6	Ind-DMSO-4	-0.36496	-0.01298	-0.28218
7	Ind-DMSO-5	-0.30053	0.04623	-0.34639
8	Ind-DMSO-6	-0.29443	0.00593	-0.38849
9	Ind-DMSO-7	-0.19012	-0.04405	-0.27247

Funding information Financial support from the Department of Chemistry and BioChemistry, Georgia Southern University (GSU); Department of Chemistry, University of Massachusetts (UMASS), Boston; and the College Office of Undergraduate Research (COUR-GSU) is gratefully recognized.

Compliance with ethical standards

Conflict of interest The authors declare that they have no conflict of interest.

References

- Muzalevskiy VM, Serdyuk OV, Nenajdenko VG (2014) Chemistry of fluorinated indoles. Fluorine in heterocyclic chemistry, vol 1, pp 117–156
- Usachev BI (2016) J Fluor Chem 185:118–167
- Biswal S, Sahoo U, Sethy S, Kumar HKS, Banerjee M (2012) Asian J Pharm Clin Res 5:1–6
- Kaushik NK, Kaushik N, Attri P, Kumar N, Kim CH, Verma AK, Choi EH (2013) Molecules 18:6620–6662
- Török M, Abid M, Mhadgut SC, Török B (2006) Biochemistry 45: 5377–5383
- Sood A, Abid M, Hailemichael S, Foster M, Török B, Török M (2009) Bioorg Med Chem Lett 19:6931–6934
- Sood A, Abid M, Sauer C, Hailemichael S, Foster M, Török B, Török M (2011) Bioorg Med Chem Lett 21:2044–2047
- Török B, Abid M, London G, Esquibel J, Török M, Mhadgut SC, Yan P, Prakash GKS (2005) Angew Chem Int Ed 44:3086–3089
- Abid M, Török B (2005) Adv Synth Catal 347:1797–1803
- Abid M, Teixeira L, Török B (2008) Org Lett 10:933–935
- Rudnitskaya A, Huynh K, Török B, Stieglitz K (2009) J Med Chem 52:878–882
- Peerannawar S, Horton W, Kokel A, Török F, Török M, Török B (2017) Struct Chem 28:391–402
- Horton W, Peerannawar S, Török B, Török M (2019) Struct Chem 30: 23–35
- Thompson MJ, Louth JC, Ferrara S, Sorrell FJ, Irving BJ, Cochrane EJ, Meijer AJ, Chen B (2011) ChemMedChem 6:115–130
- Török B, Sood A, Bag S, Kulkarni A, Borkin D, Lawler E, Dasgupta S, Landge SM, Abid M, Zhou W, Foster M, LeVine III H, Török M (2012) ChemMedChem 7:910–919
- Gong G, Kato K (2001) J Fluor Chem 108:83–86
- Borkin D, Landge SM, Török B (2011) Chirality 23:612–616
- Zhu X, Ganeshan AJ (2002) J Org Chem 67:2705–2708
- Darehkordi A, Rahmani F, Hashemi V (2013) Tetrahedron Lett 54: 4689–4692
- Nunomoto S, Kawakami K, Yamashita Y (1990) J Chem Soc Perkin Trans 1990:111–114
- Zhu Y, Rawal VH (2012) J Am Chem Soc 134:111–114
- Sundberg RJ (1996) In: Indoles. Academic Press, London, Ch.9
- Reinecke MG, Sebastian JF, Johnson HW, Pyun C (1972) J Org Chem 37:3066–3068
- Karchava AV, Melkonyan FS, Yurovskaya MA (2012) Chem Heterocycl Comp 48:391–407
- Leitch S, Jones AJ, McCluskey A (2005) Tetrahedron Lett, vol 46, pp 2915–2918
- Santaniello E, Farachi C, Ponti F (1979) Synthesis 1979:617–618
- Li Y, Zhang L, Yuan H, Liang F, Zhang J (2015) Synlett 26:116–122
- Le Noble WJ, Morris HF (1969) J Org Chem 34:1969–1973
- Kilic H, Bayindir S, Erdogan E, Saracoglu N (2012) Tetrahedron 68:5619–5630

30. Schäfer C, Ellstrom CJ, Sood A, Alonzo J, Landge SM, Tran CD, Török B (2018) ARKIVOC part ii, pp 122–130
31. Becke AD (1988) Phys Rev A38:3098–3100
32. Lee C, Yang W, Parr RG (1988) Phys Rev B37:785–789
33. Gaussian 09, Revision A.02, Frisch MJ, Trucks GW, Schlegel HB, Scuseria GE, Robb MA, Cheeseman JR, Scalmani G, Barone V, Petersson GA, Nakatsuji H, Li X, Caricato M, Marenich A, Bloino J, Janesko BG, Gomperts R, Mennucci B, Hratchian HP, Ortiz JV, Izmaylov AF, Sonnenberg JL, Williams-Young D, Ding F, Lipparini F, Egidi F, Goings J, Peng B, Petrone A, Henderson T, Ranasinghe D, Zakrzewski VG, Gao J, Rega N, Zheng G, Liang W, Hada M, Ehara M, Toyota K, Fukuda R, Hasegawa J, Ishida M, Nakajima T, Honda Y, Kitao O, Nakai H, Vreven T, Throssell K, Montgomery, Jr. JA, Peralta JE, Ogliaro F, Bearpark M, Heyd JJ, Brothers E, Kudin KN, Staroverov VN, Keith T, Kobayashi R, Normand J, Raghavachari K, Rendell A, Burant JC, Iyengar SS, Tomasi J, Cossi M, Millam JM, Klene M, Adamo C, Cammi R, Ochterski JW, Martin RL, Morokuma K, Farkas O, Foresman JB, Fox DJ (2016) Gaussian, Inc., Wallingford CT
34. Tomasi J, Mennucci B, Cammi R (2005) Chem Rev 105:2999–3093
35. Wolinski K, Hilton JF, Pulay P (1990) J Am Chem Soc 112:8251–8260
36. Legault CY (2009) CYLview, 1.0b; Université de Sherbrooke: Sherbrooke (Québec) Canada, <http://www.cylview.org>
37. Zhou F, Liu X, Zhang N, Liang Y, Zhang R, Xin X, Dong D (2014) Org Lett 16:4693–4694
38. Ryabov AD, Polyakov VA, Talebarovskaya IK, Katkova VA, Yatsimirskii AK, Berezin IV (1988) Russ Chem Bull 37:162–167
39. Tapia O, Bertran J (2002) Solvent effects and chemical reactivity. Kluwert, New York
40. Casey BM, Eakin CA, Jiao J, Sadasivam DV, Flowers RA (2009) Tetrahedron 65:10762–10768
41. Landge SM, Borkin DA, Török B (2007) Tetrahedron Lett 48: 6372–6376
42. Lin P (2003) Trifluoroacetaldehyde. Encyclopedia of reagents for organic synthesis (e-EROS). Wiley, New York
43. Bucsi I, Török B, Marco AI, Rasul G, Prakash GKS, Olah GA (2002) J Am Chem Soc 124:7728–7736

Publisher's note Springer Nature remains neutral with regard to jurisdictional claims in published maps and institutional affiliations.